

A Comprehensive Platform for *Ex Vivo* T-cell Expansion Based on Biodegradable Polymeric Artificial Antigen-presenting Cells

Erin R Steenblock¹ and Tarek M Fahmy¹

¹Department of Biomedical Engineering, Yale University, New Haven, Connecticut, USA

Efficient T-cell stimulation and proliferation in response to specific antigens is a goal of immunotherapy against infectious disease and cancer. Manipulation of this response can be accomplished by adoptive immunotherapy involving the infusion of antigen-specific T-cell populations expanded *ex vivo* with antigen presenting cells. We mimicked physiological antigen presentation on a biodegradable microparticle constructed from poly(lactide-co-glycolide) (PLGA), a polymer system whose safety has been established for use in humans. These particles present a high density of adaptor elements for attaching both recognition ligands and co-stimulatory ligands to a biodegradable core encapsulating the cytokine interleukin-2 (IL-2). We demonstrate the utility of this system in efficient polyclonal and antigen-specific T-cell stimulation and expansion, showing that sustained release of IL-2 in the vicinity of T-cell contacts dramatically improves the stimulatory capacity of these acellular systems, as compared to the effect of exogenous addition of cytokine. This results in a 45-fold enhancement in T-cell expansion. In addition, this mode of antigen presentation skews the expansion toward the CD8⁺ T-cell phenotype. This comprehensive acellular platform, capable of delivering recognition, co-stimulatory, and cytokine signals, represents a promising new technology for artificial antigen presentation.

Received 26 July 2007; accepted 7 January 2008; published online 4 March 2008. doi:10.1038/mt.2008.11

INTRODUCTION

Adoptive immunotherapy is a procedure whereby lymphocytes are expanded *ex vivo* and reinfused back into the body to enhance therapy against viral infection,^{1,2} autoimmune disease,^{3,4} or cancer.⁵⁻⁷ While natural antigen-presenting cells (APCs), notably dendritic cells (DCs), are the most potent in initiating immune responses, their use in *ex vivo* stimulation of antigen-specific immune responses in clinical settings involving adoptive immunotherapy has been limited because of issues related to the quality, expense, and time involved in their isolation and culture.⁸ Because T-cell restriction necessitates the use of autologous dendritic cells, customized isolation must be carried out for individual patients, thereby limiting the general application of this therapy. In order to

address this issue, artificial APCs (aAPCs) based on cellular and acellular systems have been proposed and tested.^{8,9}

Cellular aAPCs have been created from human leukemia cell lines,^{10,11} insect cells,¹²⁻¹⁴ and mouse fibroblasts.^{15,16} Although physiological in nature, these systems may require genetic modifications in order to effectively present antigens, and may carry the risk for potential infection or tumorigenicity. Acellular approaches use micron-size latex, polyglycolide, or magnetic beads^{8,17-19} and lipid-based vesicles.²⁰⁻²² While these platforms may eliminate the risk of infection by utilizing synthetic constructs, many lack biocompatibility and the physiological features that can enhance antigen presentation.⁹ In addition, some acellular platforms, such as magnetic beads, skew expansion toward the CD4⁺ T-cell phenotype, with minimal effects on the CD8⁺ T-cell subset⁸ which is an important population for cancer immunotherapy.

T-cell responses are mediated by the signals received from APCs.²³ Current approaches toward engineering of aAPCs exploit both recognition signals and co-stimulatory signals in the form of specific peptide-major histocompatibility complex (peptide-MHC) complexes or antibodies that crosslink the T-cell CD3 complex (recognition) and CD28 (co-stimulation). A third signal can be provided by cytokines, which are secreted by activated APCs after T-cell encounters, and which impact expansion, survival, effector function, and memory of stimulated T cells.²³⁻²⁵ None of the current aAPC platforms takes advantage of this paracrine mode of cytokine delivery although it is a central component of physiological T-cell-APC signaling.²³ Typically, cytokines are added to cultures exogenously and administered systemically to patients after reinfusion of T cells; however, such systemic administration can be associated with acute toxicity.²⁴ In addition, cytokine withdrawal can occur when T cells are transferred from *ex vivo* culture in high-concentration interleukin-2 (IL-2) to a patient, leading to failures in T-cell persistence *in vivo*.²⁶ Currently there are no aAPC technologies that incorporate all three signals in a safe, ready-to-use system that is rapidly modifiable for antigen-specific or polyclonal T-cell expansion. This is a clear limitation in design, and we seek to address it by the approach we report here.

We demonstrate that the features of an ideal APC, as described earlier, can be incorporated into a biodegradable microparticle that facilitates efficient stimulation of T cells. The biodegradability of this system allows for encapsulation and local release of cytokines, thus mimicking the natural mode of action

Correspondence: Tarek M. Fahmy, 55 Prospect Street, Room No. 412, New Haven, Connecticut 06511, USA. E-mail: tarek.fahmy@yale.edu

of this important third signal. We show that paracrine release offers advantages over the traditional approach of adding exogenous cytokine. The ability of this system to release cytokines in a sustained manner, coupled with the ease of attaching multiple ligands, results in a durable, artificial antigen-presenting system for T-cell expansion. These aAPCs represent a true “off-the-shelf,” flexible technology that is amenable both to long-term storage and to immediate use.

RESULTS

Fabrication of PLGA aAPCs

The aAPC platform is depicted in **Figure 1**. Particles can be fabricated with varying diameters in the micro- to nanometer range, and are constructed from poly(lactide-co-glycolide) (PLGA), a polymer whose safety of use in humans has been established for the past 30 years.^{27,28} Immobilization of avidin on the surface of the particles is accomplished using an avidin–palmitate conjugate that associates with PLGA during particle synthesis,²⁹ resulting in an average avidin density of 71 $\mu\text{g}/\text{mg}$ of polymer (SD = 19 $\mu\text{g}/\text{mg}$, data not shown). Micro- and nanoparticles display similar densities of avidin on a per-mass basis. The presence of avidin allows attachment of a high density of immunologically relevant biotinylated ligands whose presentation is prolonged during polymer degradation and release of encapsulated cytokines because of the preferential association of the fatty acid–avidin conjugate with the surface of the particle.²⁹ Biotinylated MHC dimers and antibodies for recognition and co-stimulation of T cells are coupled to aAPCs immediately before use by taking advantage of the high-affinity binding between avidin and biotin. In addition to the surface presentation of ligands, previous work with PLGA micro- and nanoparticles has demonstrated success for the delivery of small molecules and proteins,^{27,30} potentially providing an important third signal for T-cell stimulation.

Both nanoparticles and microparticles were fabricated using identical formulations. Particles were created using single emulsion (microparticles) and double emulsion (micro- and nanoparticles) techniques as earlier described,³¹ and were surface-modified with avidin.²⁹ Scanning electron microscopy revealed particles with

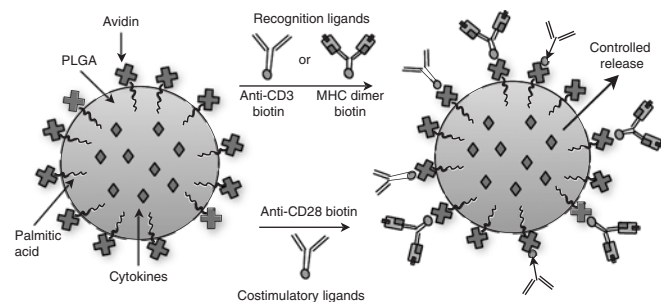


Figure 1 Schematic representation of a biodegradable artificial antigen-presenting cell (aAPC). aAPCs were fabricated using single and double emulsion techniques that allow the encapsulation of cytokines. The Avidin–palmitate conjugate was incorporated to facilitate the presentation of avidin on the particle surface. Biotinylated ligands for recognition and co-stimulation (anti-CD3, anti-CD28, and peptide-MHC complexes) were attached to aAPCs through binding to avidin presented on the aAPC. Encapsulated cytokines are released from particles in a time-dependent manner. MHC, major histocompatibility complex; PLGA, poly(lactide-co-glycolide).

average diameters of 8.0 μm and 130 nm for micro- and nanoparticles, respectively (**Figure 2a–d**). The particles were qualitatively visualized with T cells, and we observed stable interactions (**Figure 2e** and **Supplementary Figure S1**). The biocompatibility of untargeted aAPCs (particles without attached biotinylated ligands) was confirmed using a range of particle concentrations, and no effect on proliferation was observed (**Supplementary Figure S2**).

Micro-scale aAPCs enhance multivalent interactions with antigen-specific T cells as compared to nano-scale aAPCs

Biotinylated MHC-K^b dimers loaded with the cognate ovalbumin (OVA) SIINFEKL peptide OVA (OVA_{257–264})³² (SIINK^b) or noncognate OVA SIYRYYGL (SIYK^b) were coupled to micro- and nanoparticles. At the concentration of ligands used in these studies (1 μg of antibody/mg polymer or 5 μg MHC/mg polymer), 90% of the protein added was successfully bound to particles (**Supplementary Figure S3**).

In order to assess the optimal concentration of particles to be used with T cells, aAPCs were titrated beginning at 5 mg/ml and incubated with purified CD8⁺ T cells from OT-I mice, a class-I

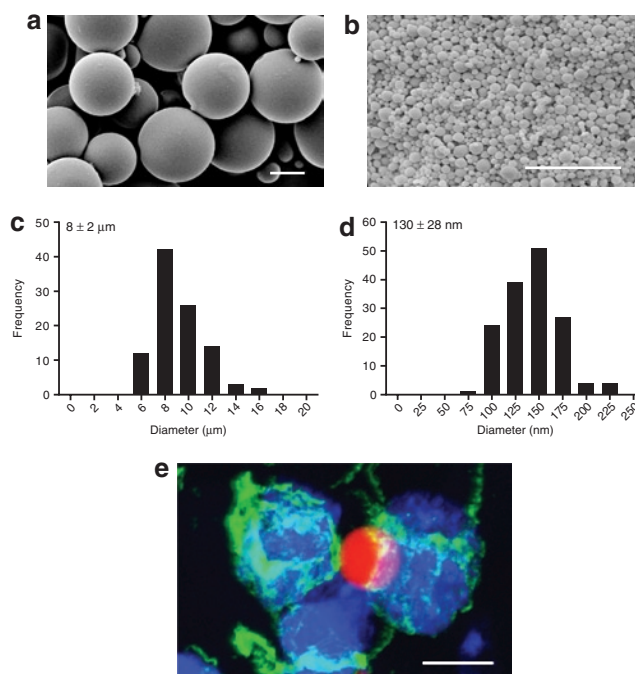


Figure 2 Characterization of artificial antigen-presenting cells (aAPCs). Scanning electron microscopy was used to view the morphology of (a) micro- and (b) nano-scale particles. Scale bars = 5 μm . Particle sizing was performed on SEM images using NIH ImageJ software. $n = 150$ particles. Size distributions are shown for (c) micro- and (d) nanoparticles, with mean diameters shown in the upper left corner of each plot. (e) aAPC–T-cell binding was visualized by immobilizing B3Z cells to poly-L-lysine-coated cover slips, which were washed three times and blocked, and then incubated with a 5 mg/ml solution of targeted microparticle aAPCs containing encapsulated Rhodamine B and surface-bound anti-CD3 and anti-CD28 for 1 hour at 4°C. After incubation, the cover slips were rinsed to remove unbound particles, and the cells were stained with phalloidin–fluorescein isothiocyanate and 4',6'-diamidino-2-phenylindole. Scale bar = 10 μm . The image shown is representative of multiple experiments.

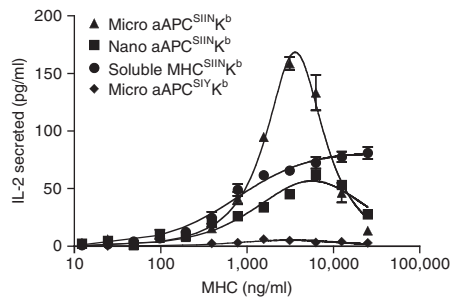


Figure 3 Micro-scale artificial antigen-presenting cells (aAPCs) are better T-cell stimuli than nano-scale aAPCs. Interleukin-2 (IL-2) secretion was measured by enzyme-linked immunosorbent assay after incubating aAPCs for 60 hours with OT-I CD8⁺ T cells at various concentrations of the stimulant at 37°C. Microparticles with attached SIIN^{K^b} (triangles) as well as nanoparticles with SIIN^{K^b} (squares) and soluble MHC^{SIIN^{K^b}} (circles) were titrated beginning at 5 mg/ml particles (5 μg/ml antibody), (a 1:1 ratio of cells:aAPCs), prior to addition of 1 × 10⁵ T cells/ml. Negligible levels of IL-2 secretion were produced in response to microparticle aAPCs presenting noncognate ligand SIY^{K^b} (diamonds). Curve fits are made to a receptor cross-linking model (see Materials and Methods). Error bars represent SEM, n = 3.

restricted T-cell line recognizing the SIINFEKL peptide presented within the context of H-2K^b. Activation was assessed by measuring IL-2 levels from cell culture supernatant. We observed that optimal stimulation occurs at an intermediate aAPC concentration, beyond which T-cell IL-2 secretion declines (Figure 3). The data were fitted to a well-established model that accounts for the biophysical aspects of this trend,³³ and model fit parameters are given in **Supplementary Table S1**. This model predicts that activation of immune cells by multivalent ligands will exhibit a bell-shaped concentration dependence curve, because of receptor aggregation on the surface of the cells.^{33,34} In this model, the decreased response at high ligand concentrations is a result of less efficient aggregation between ligands and receptors. Earlier work has reported similar trends showing symmetric, bell-shaped, non-saturating concentration dependence curves when utilizing multivalent constructs for the stimulation of T cells.^{20,34,35}

Both micro- and nanoparticles exhibit bell-shaped curves, but the stimulation maximum for microparticle aAPCs occurs at a lower concentration of constructs than the maximal response from nanoparticle aAPCs (Figure 3). In addition to the shift in optimal concentration, peak levels of IL-2 secretion were much higher in response to microparticle aAPCs when compared with nanoparticle aAPCs. These findings are supported by those of previous reports, demonstrating that micron-sized particles, which are close in size to T cells, provide optimal T-cell stimulation.³⁶ From the peak of the curve in Figure 3, we deduced that for this aAPC system, a ratio of 1:8 (particles:T cells) is optimal for stimulation.

Addition of co-stimulatory signals to aAPCs further increases T-cell stimulation

aAPCs were prepared with anti-CD28 and anti-CD3 for polyclonal activation, or with SIIN^{K^b} and anti-CD28 for antigen-specific activation. IL-2 and interferon-γ (IFN-γ) secretion as well as T-cell proliferation were assessed in order to determine activation and function of the cells. In the absence of co-stimulation,

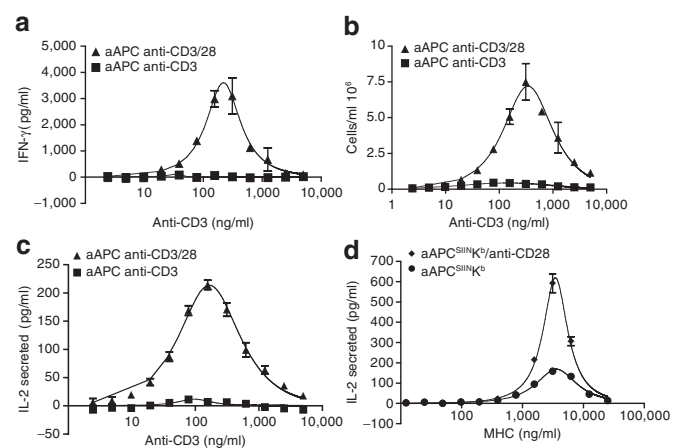


Figure 4 Addition of anti-CD28 to the artificial antigen-presenting cell (aAPC) surface further increases T-cell stimulation. Primary B6 splenocytes (5 × 10⁵ cells/ml) were stimulated by microparticle aAPCs (titrated beginning at 5 mg/ml particles (5 μg/ml antibody), a 1:1 ratio of cells:aAPCs, presenting anti-CD3 alone (squares) or anti-CD3 and anti-CD28 at a 1:1 molar ratio (triangles) for 60 hours at 37°C. (a) Interferon-γ (IFN-γ), (b) proliferation (assessed by the CellTiter-Blue Viability Assay), and (c) IL-2 secretion were measured. (d) Data were also collected for antigen-specific stimulation of OT-I CD8⁺ T cells (1 × 10⁵ T cells/ml) by microparticle aAPCs with attached SIIN^{K^b} (circles) or SIIN^{K^b} and anti-CD28 at a 1:1 molar ratio (diamonds). Error bars represent SEM, n = 3.

C57BL/6 (B6) T cells secreted minimal IL-2 and IFN-γ and failed to proliferate significantly (Figure 4a–c). The addition of anti-CD28 induced robust cytokine secretion and enhanced proliferation. Similarly, antigen-specific stimulation was increased by a fourfold enhancement in IL-2 secretion after the addition of co-stimulatory molecules to the aAPC surface (Figure 4d). These results are consistent with earlier studies that used polystyrene latex microspheres for T-cell stimulation,³⁷ and show that incorporation of co-stimulatory molecules on the particle surface improves T-cell expansion.

Controlled release of rhIL-2 from biodegradable aAPCs enhances T-cell expansion in a concentration-dependent manner

The delivery of IL-2 increases the viability and proliferative capacity of T cells.³⁸ A distinct advantage of the current platform is its ability to encapsulate and release cytokines such as IL-2 in a sustained fashion. The release of the cytokine can be controlled by varying the particle preparation conditions. In order to demonstrate these features, recombinant human IL-2 (rhIL-2) was encapsulated in microparticles using three methods: (i) in phosphate-buffered saline (PBS) using a double emulsion water-in-oil-in-water technique (low encapsulation with burst release); (ii) as a lyophilized solid using a single emulsion solid-in-oil-in-water (s/o/w) technique (medium encapsulation with burst); (iii) by first stabilizing with trehalose, a known preservation agent,³⁹ then encapsulating using a single emulsion s/o/w technique (high encapsulation and sustained release). In control experiments trehalose had neither a stimulatory nor an inhibitory effect on T-cell activation (Supplementary Figure S4). The kinetics of controlled release of rhIL-2 from each type of microparticle aAPC in PBS are shown in Figure 5a. Controlled

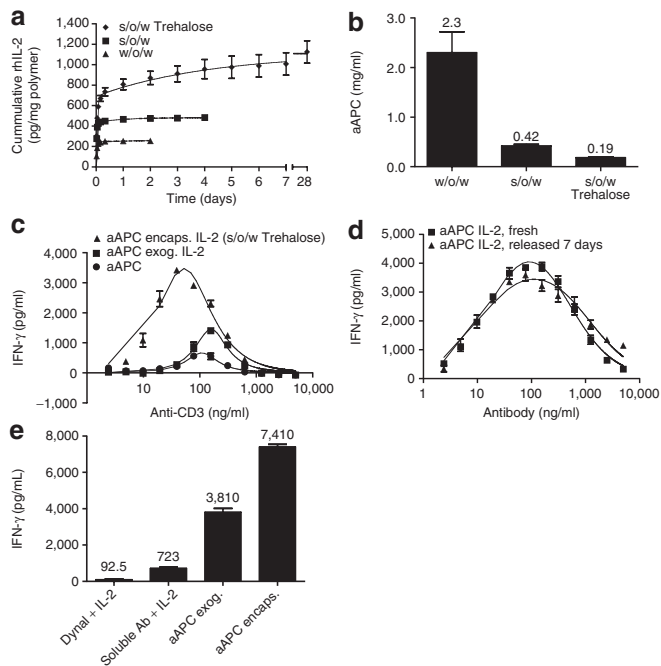


Figure 5 Level of interleukin-2 (IL-2) release from biodegradable particles correlates with T-cell stimulation. **(a)** The release of encapsulated rhIL-2 from 10 mg of various microparticle formulations [diameter = 8 μ m, high (diamonds), medium (squares), and low (triangles)] was measured in 1 ml of phosphate-buffered saline by enzyme-linked immunosorbent assay. **(b)** The effect of delivering rhIL-2 from microparticle artificial antigen-presenting cells (aAPCs) was investigated by stimulating B6 splenocytes (5×10^5 cell/ml) for 60 hours at 37°C. aAPCs presenting anti-CD3 and anti-CD28 with varying IL-2 loads (depending upon the method of encapsulation) were titrated in order to determine the optimal concentration for stimulating interferon- γ (IFN- γ) production by B6 splenocytes. The concentration of aAPCs for which peak IFN- γ secretion occurs is shown for each formulation. **(c)** The stimulation of B6 splenocytes by aAPCs with encapsulated IL-2 (triangles) was compared with the corresponding stimulative effects of aAPCs with exogenous addition of the cytokine (squares), and aAPCs without IL-2 (circles). The titration of all groups began at 5 mg/ml of microparticles (antibody concentration of 5 μ g/ml). **(d)** Splenocytes were stimulated by aAPCs displaying anti-CD3 and anti-CD28. The aAPCs were either freshly prepared (squares) or allowed to release cytokine in phosphate-buffered saline (PBS) at 37°C for 7 days and then washed before the antibodies were loaded (triangles). **(e)** Stimulation by aAPCs with encapsulated IL-2 was compared with stimulation by aAPCs with exogenous IL-2, aAPCs with soluble antibody plus IL-2 of equivalent concentrations, and Dymal magnetic beads coated with avidin and IL-2. Error bars represent SEM, $n = 3$. Data in **a** are fitted to a two-phase exponential association function.

release curves were obtained from 10 mg of particles without attached biotinylated ligands. The attachment of surface ligands does not affect the release characteristics.²⁹ The resulting biphasic plots are typical of protein release during PLGA particle degradation and are characterized by an initial burst release followed by continual release of protein over time.⁴⁰

In order to examine the effects of varying rhIL-2 loading on T-cell stimulation, B6 splenocytes were stimulated in a polyclonal manner by aAPCs fabricated with different rhIL-2 loading (“loaded IL-2 aAPCs”) presenting anti-CD3 and anti-CD28. As expected, peak stimulation was observed with lower aAPC concentrations encapsulating higher levels of rhIL-2, releasing gradually (Figure 5b).

Furthermore, this mode of stimulation seemed to be more efficient than exogenous addition of IL-2. In order to demonstrate this effect, IL-2-loaded aAPCs (s/o/w trehalose-high) were compared with unloaded aAPCs in the presence and absence of equal concentrations of exogenous, titrated rhIL-2 (5 ng/ml at highest concentration). While the addition of exogenous rhIL-2 produced a moderate increase in IFN- γ secretion, paracrine delivery of rhIL-2 more than doubled this response (Figure 5c). In order to determine whether this effect is caused by the burst of cytokine from the particle observed at early time points or by sustained release over time, the particles were allowed to release rhIL-2 at 37°C for 7 days, and were then washed and coupled to antibodies before T-cell stimulation. As shown in Figure 5d, cells exhibited only moderate decreases in IFN- γ secretion even when the burst release of cytokine was washed away before T-cell stimulation. This supports the hypothesis that gradual release of cytokine from the aAPC during the stimulation period has significant effects on the magnitude of stimulation.

Next, we compared the performance of this system with soluble antibodies and a commercially available aAPC platform, 4 μ m Dymal beads (at equivalent particle concentrations) loaded with anti-CD3 and anti-CD28, in the presence of exogenous rhIL-2 (Figure 5e). Soluble antibody and Dymal beads induced lower IFN- γ secretion than both loaded and exogenous rhIL-2 aAPCs, and appeared to require higher concentrations in order to achieve peak stimulation. Reported values for the optimal stimulation of T cells with Dymal beads suggest that a 3:1 ratio of beads to cells is ideal.⁴¹ In our study, optimal stimulation with loaded IL-2 aAPCs was achieved with a 1:64 (aAPC:T-cell ratio) for polyclonal expansion (Figure 5c and d).

For T-cell expansion, paracrine delivery of rhIL-2 from aAPCs is more efficient than exogenous addition

In order to examine the effect of paracrine rhIL-2 delivery on T-cell expansion, carboxyfluorescein diacetate succinimidyl ester (CFSE) dye-labeled B6 splenocytes were monitored during polyclonal stimulation. Only loaded IL-2 aAPCs produced near-complete division of T cells after 4 days of culture (Figure 6a). Soluble antibodies and unloaded aAPCs were not as efficient in facilitating T-cell division even with a tenfold increase in the level of exogenous rhIL-2. In addition, we observed significant improvements in the absolute number of cells expanded with IL-2 loaded aAPCs. After 1 week of culture without restimulation, B6 splenocytes showed a 45-fold expansion in absolute cell numbers in comparison with other methods for stimulation (Figure 6b).

Polyclonal expansion of T cells by aAPCs led to an increase in the proportion of CD8⁺ T cells. The addition of exogenous rhIL-2 to cultures containing unloaded aAPCs did not produce CD8⁺ CFSE^{Low} populations equal to those of loaded IL-2 aAPCs (Figure 6c). Increasing the concentration of exogenous rhIL-2 improved stimulation, but expansion remained less than in cells treated with loaded IL-2 aAPCs. Only an increase in the concentrations of soluble antibody and rhIL-2 by an order of magnitude produced effects comparable with those produced by loaded IL-2 aAPCs (Figure 6d). Analogous results were observed with antigen-specific stimulation, with the percentage

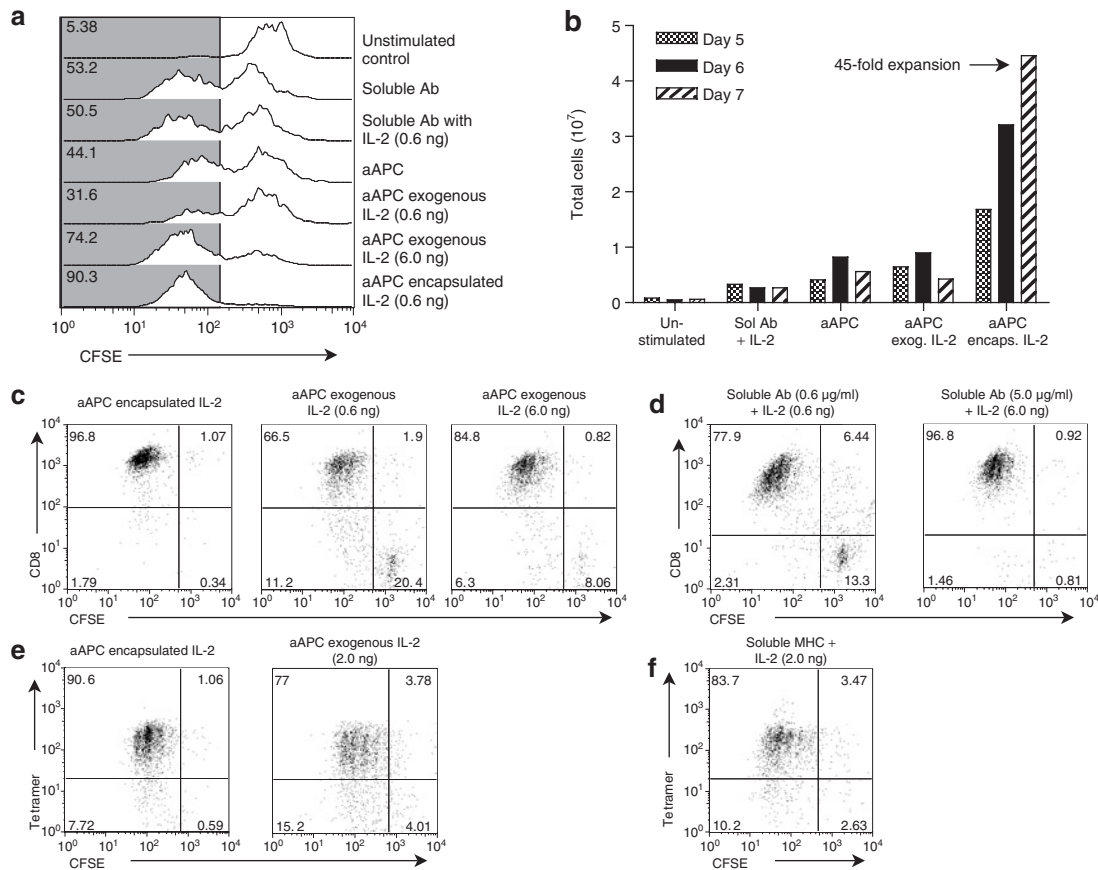


Figure 6 Paracrine delivery of interleukin-2 (IL-2) increases T-cell expansion as compared to exogenous IL-2 addition. **(a)** Cell division of B6 splenocytes stimulated in a polyclonal manner was assessed by monitoring carboxyfluorescein diacetate succinimidyl ester (CFSE) dye dilution after 4 days of culture. The numbers in the upper left of each histogram represent the percentage of divided cells as defined by the gray gate. The data shown are gated on the total lymphocyte population. **(b)** Absolute cellular expansion was followed *in vitro* using a Multisizer 3 Coulter counter (Beckman Coulter). B6 splenocytes (1×10^6 cells/ml) were stimulated by soluble antibody or artificial antigen-presenting cells (aAPCs), and culture aliquots were removed for enumeration on days 5, 6, and 7. **(c)** In order to examine the subset of cells expanded by each method, CFSE-labeled B6 splenocytes or OT-I CD8⁺ T cells (1×10^6 cells/ml) were cultured for 4 days with aAPCs, either loaded or not loaded with IL-2 (0.3 mg/ml). Loaded IL-2 aAPCs with anti-CD3/anti-CD28 were compared with equivalent concentrations of unloaded aAPCs in the presence of exogenous IL-2. **(d)** Soluble antibodies, and The data are representative of three independent experiments. **(e)** Antigen-specific stimulation of OT-I CD8⁺ T cells was performed as in **c**, and T cells were stained with phycoerythrin-labeled ^{SIIN}K^b tetramer. **(f)** Soluble major histocompatibility complex (MHC) dimers were also used for comparison. **(e)** and **(f)** major histocompatibility complex (MHC) dimers were also used for comparison. encaps., encapsulated; exog., exogenous.

of ^{SIIN}K^b-tetramer-positive CFSE^{Low} cells being the greatest after stimulation with loaded IL-2 aAPCs (Figure 6e and f).

aAPCs increase the sensitivity of T cells to IL-2 and selectively expand CD8⁺ cells

CD25, the α -chain of the IL-2 receptor, is an established activation marker that is upregulated when *in vitro* T-cell stimulation occurs.⁴² It was found that the expression of CD25 increased with each of the stimulation methods, but was even further upregulated on cells that had been exposed to loaded IL-2 aAPCs (Figure 7a). In addition, subset T-cell analysis revealed that loaded IL-2 aAPCs preferentially expanded CD8⁺ T cells with near 100% selectivity during polyclonal expansion (Figure 7b). This is in contrast to the results obtained from other methods of stimulation investigated in this work, including commercially available magnetic beads. Unloaded aAPCs with and without rhIL-2 produced near-equal proportions of CD4⁺ and CD8⁺ T cells, whereas soluble antibodies and Dynal beads (used at a 3:1 ratio of beads:cells), in the presence or absence of exogenous rhIL-2, selectively expanded CD4⁺

T cells. These results are in agreement with findings from earlier studies, demonstrating that some aAPC platforms, both cellular and acellular, preferentially expand CD4⁺ T cells.^{9,43} T cells that are expanded with loaded IL-2 aAPCs are functional and activated, as inferred from the upregulation of the activation markers CD25, CD44, and CD69 (Figure 7c).

DISCUSSION

The novel system presented in this study embodies several key features of an ideal aAPC for use in adoptive immunotherapy. First, the ideal aAPC should be easily modifiable to accommodate a variety of ligands. Second, it would be desirable for this ideal aAPC to release cytokines in a tunable manner at the site of interactions with T lymphocytes. While exogenous addition of a cytokine is a simple strategy to augment signaling *in vitro*, we have demonstrated that paracrine signaling through aAPCs, made possible by the degradable nature of our aAPCs, is a much more effective strategy, because it enhances expansion at a lower concentration of potentially toxic cytokines, and selectively expands

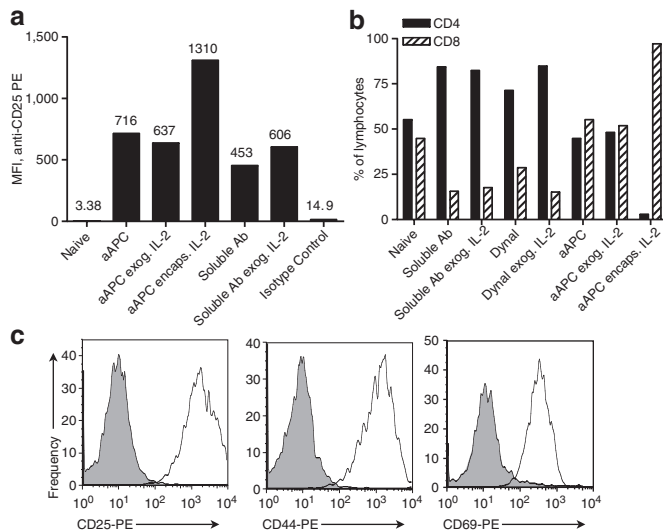


Figure 7 Paracrine delivery of interleukin-2 (IL-2) from biodegradable artificial antigen-presenting cells (aAPCs) increases IL-2R expression and selectively expands the CD8⁺ T-cell subset. B6 splenocytes were stimulated by various aAPC configurations for 4 days at 37 °C. **(a)** Flow cytometry was performed on a BD FACScan to determine anti-CD25-PE mean fluorescence intensity after gating on CD8⁺ T cells. **(b)** Cells were stained for CD4 and CD8 to determine the relative proportions of each lymphocyte subset after polyclonal expansion by various methods. **(c)** Cells stimulated by loaded IL-2 aAPCs were stained for the activation markers CD25, CD44, and CD69. Isotype controls are shown in gray. The data in **a** and **c** are gated on CD8⁺ T cells. The results are representative of three independent experiments. Ab, antibody; encaps., encapsulated; exog., exogenous; PE, phycoerythrin.

CD8⁺ T cells. Third, the ideal system should enable stable storage and ensure safety in the event of accidental injection.

Professional APCs such as dendritic cells can be viewed as micron-sized biological objects assembled from nano-scale units, which are highly optimized for interaction with T cells. Biodegradable polymer particulates, as described in this report, are well suited for the design of an aAPC that is both easily generalized and highly optimized, possessing the essential features of professional cellular aAPCs with additional attractive properties such as: (i) control over the size-range of fabrication, from tens of microns down to 100 nm or lower; (ii) reproducible biodegradability without the addition of enzymes or cofactors;⁴⁴ (iii) capability for sustained release of encapsulated, protected cytokine factors that may be tuned from days to months by varying preparation conditions or factors such as the PLA:PGA copolymer ratio;⁴⁵ (iv) well-understood fabrication methodologies offering flexibility in respect of many parameters, including choice of polymer, solvent, stabilizer, and scale of production; and (v) control over the introduction and sustained presentation of modular functionalities onto the aAPC surface.²⁹

The system described in this work highlights a new finding regarding the value of paracrine cytokine delivery for T-cell stimulation and expansion. The increased potency of rhIL-2 delivered in a paracrine, sustained manner allows the use of smaller amounts of cytokine to achieve greater T-cell activation and expansion as compared to exogenous cytokine addition. This increased responsiveness of T cells to controlled rhIL-2 release from aAPCs could be the result of two possible mechanisms.

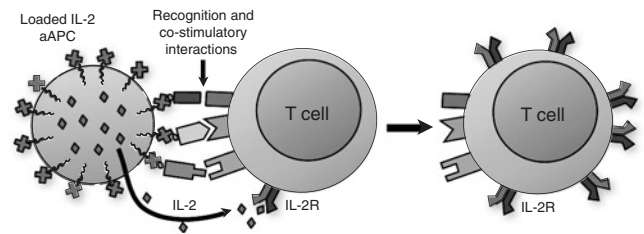


Figure 8 Proposed mechanism for enhancement of T-cell expansion by paracrine delivery of interleukin-2 (IL-2). Proximal contact of T cells with IL-2-loaded artificial antigen-presenting cells (aAPCs) results in sustained paracrine IL-2 signaling. Paracrine signaling sensitizes the T cell to IL-2, leading to an upregulation of the IL-2 receptor, CD25, on the surface of T cells.

In the first of these possible mechanisms, the released IL-2 associates with the particle surface nonspecifically, presenting the cytokine in a manner that enhances its activity: a conversion of the IL-2 to a “superagonist” similar to what has been shown by Sprent and colleagues using antibodies to IL-2.⁴⁶ The second possible mechanism is based upon the simple fact that proximity of presentation results in better capture of released IL-2, thereby facilitating enhanced T-cell responsiveness.⁴⁷ In order to distinguish between these mechanisms, we note that particles incubated with exogenous rhIL-2 do not stimulate as effectively as rhIL-2 that is released from within (**Figures 5c** and **6a–f**). In addition, particles from which excess IL-2 (that may be associated with the surface) have been thoroughly washed away are only slightly less effective than unwashed particles (**Figure 5d**). These observations argue against the “superagonist” mechanism and suggest a proximity effect model wherein the sustained release of rhIL-2 by aAPCs in proximity to T cells increases its local concentration and sensitizes the cells to the presence of IL-2 through upregulation of CD25. This process is demonstrated in **Figure 7a**. A schematic of this proposed mechanism is depicted in **Figure 8**. Stimulation of T cells in this manner results in selective expansion of the CD8⁺ T-cell subset (**Figure 7b**). This offers distinct advantages with regard to efficiency and time, as no separation step is required to enrich for CD8⁺ cells.

A practical advantage of the acellular aAPC described here is its potential for long-term storage and transportation without loss of integrity. We have found that assembled aAPCs retain their stimulatory capacity for at least 1 week when stored at 4 °C (**Supplementary Figure S5**). This, combined with the tunability of the platform, ensures the potential for widespread use in a number of therapeutic and investigative application-specific configurations.

MATERIALS AND METHODS

Cell lines and primary cells. Animal studies were approved by the Institutional Animal Care and Use Committee at Yale University (New Haven, CT). All animals were routinely used at 6–8 weeks of age, were maintained under specific pathogen-free conditions, and were routinely checked by personnel from the Yale University Animal Resource Center. C57BL/6 (B6) mice were obtained from Jackson Laboratories (Bar Harbor, ME). OT-I TCR transgenic breeder mice were a generous gift from Ruslan Medzhitov (Yale University) and were bred heterozygously on a B6 background in our animal facility. Phenotypes were screened using V- α 2 and CD8 α antibodies (eBioscience, San Diego, CA). B3Z hybridoma cells with

T-cell receptor specific for SIINFEKL peptide (OVA₂₅₇₋₂₆₄) were a generous gift from Peter Cresswell (Yale University) and were maintained in Rosewell Park Memorial Institute (RPMI)-1640 (Invitrogen, Carlsbad, CA) medium supplemented with 10% fetal bovine serum (Atlanta Biologicals, Lawrenceville, GA) and 2% penicillin–streptomycin (Sigma Aldrich, St. Louis, MO). Primary splenocytes were obtained from homogenized naive mouse spleens after depletion of erythrocytes by hypotonic lysis (Acros Organics, Geel, Belgium). Splenocytes were resuspended in complete RPMI-10 medium, consisting of RPMI-1640 supplemented with 10% fetal bovine serum, 2 mmol/l L-glutamine (Invitrogen, Carlsbad, CA), 25 μmol/l β-mercaptoethanol (American Bioanalytical, Natick, MA), 2% penicillin–streptomycin and 1% gentamicin (Sigma Aldrich, St. Louis, MO). B6 splenocytes were used without further purification, while OT-I CD8⁺ T cells were isolated by negative immunoselection (R&D Systems, Minneapolis, MN).

Fabrication of biodegradable aAPCs. PLGA 50/50 with an average molecular weight of 80 kd was obtained from Durect Corporation (Cupertino, CA). Microparticles were fabricated using a single emulsion s/o/w technique or a double emulsion water-in-oil-in-water technique, while nanoparticles were created using a double emulsion water-in-oil-in-water technique.³¹ Both micro- and nanoparticles were surface-modified with avidin–palmitate conjugate as described previously.²⁹ For cytokine encapsulation, 100 μg of rhIL-2 (obtained as a generous gift from Maria Parkhurst, National Cancer Institute) was lyophilized with or without a tenfold excess by mass of trehalose (Sigma Aldrich, St. Louis, MO), and incorporated as a solid during fabrication (s/o/w single emulsion technique) or added in 100 μl of PBS (water-in-oil-in-water emulsion technique) without trehalose. The particles were lyophilized and stored at –20 °C until use.

Characterization of biodegradable aAPCs. The particles were imaged using scanning electron microscopy. Images were analyzed with NIH ImageJ to determine the size distribution of particle diameters by counting at least 150 particles/sample. For loaded IL-2 aAPCs, a controlled release profile was obtained in 1 ml PBS at 37 °C from 10 mg of particles. Enzyme-linked immunosorbent assay analysis was performed to measure rhIL-2 levels (BD Biosciences, San Jose, CA). The density of avidin on the particle surface was determined using the micro bicinchoninic acid assay (Pierce, Rockford, IL) in accordance with the manufacturer's instructions, with the exception that particles were removed by centrifugation before absorbance readings were performed.

Ligand coupling to the particle surface. Biotinylated anti-mouse CD3ε (BD Biosciences, San Jose, CA) or biotinylated peptide-loaded MHC-K^b-Ig dimers (obtained as a generous gift from Jonathan Schneck, Johns Hopkins University)⁴⁸ and anti-mouse CD28 (BD Biosciences, San Jose, CA) were added at 10 μg/ml to a 10 mg/ml solution of PLGA particles in PBS and rotated at room temperature for 20 minutes. Particles were washed with PBS + 1% fetal bovine serum and resuspended in complete RPMI-10 medium. Anti-CD28, when present, was added at a 1:1 molar ratio to anti-CD3 or MHC-K^b-Ig.

T-cell stimulation studies. aAPCs coated with antibody or MHC were titrated across rows of a round-bottom 96-well plate (BD Biosciences, San Jose, CA) in 100 μl of media per well. Equal masses of micro- and nanoparticles were used, beginning with a maximum concentration of 5 mg/ml. B6 splenocytes or OT-I CD8⁺ T cells were added to each well at a final concentration of 5 × 10⁵ cells/ml (B6) or 1 × 10⁵ (OT-I). Nonbiodegradable Dynal beads (4 μm diameter; Invitrogen, Carlsbad, CA) were used at a concentration of beads equal to the PLGA microparticle concentrations (1 × 10⁵ microparticles/mg of polymer). In all cases, the highest concentration of aAPCs or beads corresponded to a 1:1 ratio of cells:particles, and the highest antibody concentration was 5 μg/ml. After incubation at 37 °C for 60 hours, plates were centrifuged at 1,500 rpm for 7 minutes in a table top centrifuge, and the supernatant was removed for IFN-γ enzyme-linked

immunosorbent assay analysis or mL-2 enzyme-linked immunosorbent assay. Cell pellets were resuspended in media and analyzed for viability using Cell Titer Blue (Promega, Madison, WI). For burst release studies, aAPCs were allowed to release IL-2 in PBS at 37 °C for 7 days prior to coupling to biotinylated anti-CD3 and anti-CD28 and use in stimulation studies. For stability studies, assembled aAPCs were incubated at 4 °C for 1 week before use. The values reported were obtained by using dilutions of supernatant that yielded absorbance values within the linear portion of the standard curve.

Fluorescence microscopy. B3Z cells were washed twice in PBS to remove serum proteins before being incubated with poly-L-lysine-coated cover slips (BD Biosciences, San Jose, CA). 1 × 10⁶ cells/ml were added in serum-free RPMI-1640 at 37 °C for 1 hour. The cover slips were then blocked in RPMI-10 medium for 10 minutes at room temperature. aAPCs with encapsulated Rhodamine B (Acros Organics, Geel, Belgium) and attached anti-CD3 and anti-CD28 were added to cover slips at 5 mg/ml in RPMI-10. Following a 1-hour incubation at 4 °C, cover slips were washed and fixed with 4% paraformaldehyde (USB, Cleveland, OH) for 10 minutes at room temperature. After fixing, the cells were permeabilized and stained with phalloidin–fluorescein isothiocyanate (Invitrogen, Carlsbad, CA) and Vectashield with 4',6-diamidino-2-phenylindole (Vector Laboratories, Burlingame, CA). Slides were visualized using a Leica SP5 confocal microscope (Leica Microsystems, Bannockburn, IL).

Assessment of expansion by flow cytometry. CFSE-labeled B6 splenocytes or OT-I CD8⁺ T cells (2 × 10⁶ cells) were exposed to various concentrations of soluble ligands (anti-CD3 for polyclonal stimulation, and ^{SIN}K^b dimers for antigen-specific stimulation (anti-CD28 was present in both cases at a 1:1 molar ratio), or ligand-coated aAPCs in the presence or absence of rhIL-2 and trehalose. Antibodies and rhIL-2 were added to achieve the indicated final concentrations in 2 ml of media. aAPCs were added at 0.3 mg/ml final concentration (40:1 cells:aAPCs). Dynal beads were used at a 3:1 ratio of beads:cells with concentrations of antibody equal to those of aAPCs. All antibodies, aAPCs, rhIL-2, and trehalose were added at the beginning of the experiment with no restimulation during the course of the study. Cell aliquots were obtained on day 4, and flow cytometric analysis was performed using a Becton Dickinson FACScan instrument (San Jose, CA) and FlowJo software (Tree Star, Ashland, OR). Splenocytes were stained with a 1:200 dilution of anti-CD8 phycoerythrin and OT-I CD8⁺ T cells were stained with a 1:20 dilution of phycoerythrin-labeled ^{SIN}K^b tetramer (Beckman Coulter, Fullerton, CA). Analysis of fluorescence was performed after gating on the lymphocyte population in side scatter versus forward scatter plots, and, where noted, the CD8⁺ subset. Staining for activation markers was performed using anti-CD25, anti-CD44, and anti-CD69, all phycoerythrin-labeled, and subset analysis was carried out using anti-CD4 fluorescein isothiocyanate and anti-CD8 phycoerythrin. All antibodies were obtained from BD Biosciences (San Jose, CA). In order to measure absolute cellular expansion of splenocyte cultures, the cells were analyzed on a Multisizer3 (Beckman Coulter, Fullerton, CA) at dilutions within the working range of the instrument. Particle counts were independently measured and subtracted from samples undergoing aAPC stimulation.

Data fitting and statistical analysis. Data fitting was performed using GraphPad Prism 4.0 (GraphPad Software, San Diego, CA). Controlled release data were fitted to a two-phase exponential association model, and stimulation data were fitted to a receptor cross-linking model³³ where the equation of fit is given by

$$\text{Response} = \frac{P_1 \delta}{1 + P_2 \delta} \quad \text{where} \quad \delta = \frac{C_{\max} C}{(C_{\max} + C)^2}$$

C is the independent variable, concentration of ligand, C_{max} is the ligand concentration at which a maximal response is observed, and P₁ and P₂ are parameters relating to the height and width of the curve.

See also **Supplementary Materials and Methods.**

ACKNOWLEDGMENTS

We thank Maria Parkhurst and Steven Rosenberg at the National Cancer Institute for their generous gift of rHL-2. We also thank Jonathan Schneck (Johns Hopkins University) for his generous gift of MHC-Ig dimers used in this work. The authors would like to acknowledge Mark Saltzman (Yale University), Jordan Pober (Yale University), and Daniel Goldstein (Yale University) for helpful discussions. We also thank Peter Cresswell (Yale University) and Ruslan Medzhitov (Yale University) for kindly providing cell lines and transgenic mice. The assistance of C. Bradford Calloway (Leica Microsystems) with confocal microscopy and Don Foster (Yale University) with flow cytometry are greatly appreciated. Partial funding was provided by The US Department of Homeland Security (predoctoral fellowship to E.R.S.). The authors declare no competing financial interests.

SUPPLEMENTARY MATERIAL

Figure S1. aAPCs interact specifically with T cells.

Figure S2. Biodegradable aAPCs are nontoxic to T cells *in vitro*.

Figure S3. Antibody binds to micro and nano-scale aAPCs.

Table S1. Summary of model fit parameters.

Figure S4. Trehalose does not impact T-cell stimulation.

Figure S5. Stability of assembled aAPCs.

Materials and Methods.

REFERENCES

- Papadopoulos, EB, Ladanyi, M, Emanuel, D, Mackinnon, S, Boulad, F, Carabasi, MH *et al.* (1994). Infusions of donor leukocytes to treat Epstein-Barr virus-associated lymphoproliferative disorders after allogeneic bone marrow transplantation. *N Engl J Med* **330**: 1185–1191.
- Savoldo, B, Heslop, HE and Rooney, CM (2000). The use of cytotoxic T cells for the prevention and treatment of Epstein-Barr virus induced lymphoma in transplant recipients. *Leuk Lymphoma* **39**: 455–464.
- Hori, S, Takahashi, T and Sakaguchi, S (2003). Control of autoimmunity by naturally arising regulatory CD4⁺ T cells. *Adv Immunol* **81**: 331–371.
- Karim, M, Kingsley, CI, Bushnell, AR, Sawitzki, BS and Wood, KJ (2004). Alloantigen-induced CD25⁺CD4⁺ regulatory T cells can develop *in vivo* from CD25-CD4⁺ precursors in a thymus-independent process. *J Immunol* **172**: 923–928.
- Dudley, ME and Rosenberg, SA (2003). Adoptive-cell-transfer therapy for the treatment of patients with cancer. *Nat Rev Cancer* **3**: 666–675.
- Riddell, SR, Murata, M, Bryant, S, Warren, EH (2002). T-cell therapy of leukemia. *Cancer Control* **9**: 114–122.
- Yee, C, Thompson, JA, Byrd, D, Riddell, SR, Roche, P, Celis, E *et al.* (2002). Adoptive T cell therapy using antigen-specific CD8⁺ T cell clones for the treatment of patients with metastatic melanoma: *in vivo* persistence, migration, and antitumor effect of transferred T cells. *Proc Natl Acad Sci USA* **99**: 16168–16173.
- Oelke, M, Maus, MV, Didiano, D, June, CH, Mackensen, A and Schneck, JP (2003). *Ex vivo* induction and expansion of antigen-specific cytotoxic T cells by HLA-Ig-coated artificial antigen-presenting cells. *Nat Med* **9**: 619–624.
- Kim, JV, Latouche, JB, Riviere, I and Sadelain, M (2004). The ABCs of artificial antigen presentation. *Nat Biotechnol* **22**: 403–410.
- Hirano, N, Butler, MO, Xia, Z, Berezovskaya, A, Murray, AP, Ansen, S *et al.* (2006). Efficient presentation of naturally processed HLA class I peptides by artificial antigen-presenting cells for the generation of effective antitumor responses. *Clin Cancer Res* **12**: 2967–2975.
- Maus, MV, Thomas, AK, Leonard, DG, Allman, D, Addya, K, Schlienger, K *et al.* (2002). *Ex vivo* expansion of polyclonal and antigen-specific cytotoxic T lymphocytes by artificial APCs expressing ligands for the T-cell receptor, CD28 and 4-1BB. *Nat Biotechnol* **20**: 143–148.
- Mitchell, MS, Darrah, D, Yeung, D, Halpern, S, Wallace, A, Voland, J *et al.* (2002). Phase I trial of adoptive immunotherapy with cytolytic T lymphocytes immunized against a tyrosinase epitope. *J Clin Oncol* **20**: 1075–1086.
- Jackson, MR, Song, ES, Yang, Y and Peterson, PA (1992). Empty and peptide-containing conformers of class I major histocompatibility complex molecules expressed in *Drosophila melanogaster* cells. *Proc Natl Acad Sci USA* **89**: 12117–12121.
- Sun, S, Cai, Z, Langlade-Demoyen, P, Kosaka, H, Brunmark, A, Jackson, MR *et al.* (1996). Dual function of *Drosophila* cells as APCs for naive CD8⁺ T cells: implications for tumor immunotherapy. *Immunity* **4**: 555–564.
- Latouche, JB and Sadelain, M (2000). Induction of human cytotoxic T lymphocytes by artificial antigen-presenting cells. *Nat Biotechnol* **18**: 405–409.
- Schoenberger, SP, Jonges, LE, Mooijaart, RJ, Hartgers, F, Toes, RE, Kast, WM *et al.* (1998). Efficient direct priming of tumor-specific cytotoxic T lymphocyte *in vivo* by an engineered APC. *Cancer Res* **58**: 3094–3100.
- Levine, BL, Mosca, JD, Riley, JL, Carroll, RG, Vahey, MT, Jagodzinski, LL *et al.* (1996). Antiviral effect and *ex vivo* CD4⁺ T cell proliferation in HIV-positive patients as a result of CD28 costimulation. *Science* **272**: 1939–1943.
- Tham, EL, Jensen, PL and Mescher, MF (2001). Activation of antigen-specific T cells by artificial cell constructs having immobilized multimeric peptide-class I complexes and recombinant B7-Fc proteins. *J Immunol Methods* **249**: 111–119.
- Shalaby, WS, Yeh, H, Woo, E, Corbett, JT, Gray, H, June, CH *et al.* (2004). Absorbable microparticulate cation exchanger for immunotherapeutic delivery. *J Biomed Mater Res B Appl Biomater* **69**: 173–182.
- van Rensen, AJ, Wauben, MH, Grosfeld-Stulemeyer, MC, van Eden, W and Crommelin, DJ (1999). Liposomes with incorporated MHC class II/peptide complexes as antigen presenting vesicles for specific T cell activation. *Pharm Res* **16**: 198–204.
- Prakken, B, Wauben, M, Genini, D, Samodal, R, Barnett, J, Mendivil, A *et al.* (2000). Artificial antigen-presenting cells as a tool to exploit the immune “synapse”. *Nat Med* **6**: 1406–1410.
- Thery, C, Zitvogel, L and Amigorena, S (2002). Exosomes: composition, biogenesis and function. *Nat Rev Immunol* **2**: 569–579.
- Pardoll, DM (2002). Spinning molecular immunology into successful immunotherapy. *Nat Rev Immunol* **2**: 227–238.
- Fyfe, G, Fisher, RI, Rosenberg, SA, Sznol, M, Parkinson, DR and Louie, AC (1995). Results of treatment of 255 patients with metastatic renal cell carcinoma who received high-dose recombinant interleukin-2 therapy. *J Clin Oncol* **13**: 688–696.
- Schluns, KS and Lefrancois, L (2003). Cytokine control of memory T-cell development and survival. *Nat Rev Immunol* **3**: 269–279.
- Riddell, SR (2007). Engineering antitumor immunity by T-cell adoptive immunotherapy. *Hematology Am Soc Hematol Educ Program* 250–256.
- Langer, R and Folkman, J (1976). Polymers for the sustained release of proteins and other macromolecules. *Nature* **263**: 797–800.
- Yamaguchi, K and Anderson, JM (1993). *In vivo* biocompatibility studies of medisorb(R) 65/35 D,L-lactide/glycolide copolymer microspheres. *J Control Release* **24**: 81–93.
- Fahmy, TM, Samstein, RM, Harness, CC and Saltzman, WM (2005). Surface modification of biodegradable polyesters with fatty acid conjugates for improved drug targeting. *Biomaterials* **26**: 5727–5736.
- Mahoney, MJ and Saltzman, WM (2001). Transplantation of brain cells assembled around a programmable synthetic microenvironment. *Nat Biotechnol* **19**: 934–939.
- Jain, RA (2000). The manufacturing techniques of various drug loaded biodegradable poly(lactide-co-glycolide) (PLGA) devices. *Biomaterials* **21**: 2475–2490.
- Hogquist, KA, Jameson, SC, Heath, WR, Howard, JL, Bevan, MJ and Carbone, FR (1994). T cell receptor antagonist peptides induce positive selection. *Cell* **76**: 17–27.
- MacClashan, DW Jr., Dembo, M and Goldstein, B (1985). Test of a theory relating to the cross-linking of IgE antibody on the surface of human basophils. *J Immunol* **135**: 4129–4134.
- Stone, JD, Cochran, JR and Stern, LJ (2001). T-cell activation by soluble MHC oligomers can be described by a two-parameter binding model. *Biophys J* **81**: 2547–2557.
- Fahmy, TM, Bieler, JG, Edidin, M and Schneck, JP (2001). Increased TCR avidity after T cell activation: a mechanism for sensing low-density antigen. *Immunity* **14**: 135–143.
- Mescher, MF (1992). Surface contact requirements for activation of cytotoxic T lymphocytes. *J Immunol* **149**: 2402–2405.
- Deeths, MJ and Mescher, MF (1997). B7-1-dependent co-stimulation results in qualitatively and quantitatively different responses by CD4⁺ and CD8⁺ T cells. *Eur J Immunol* **27**: 598–608.
- Janeway, CA, Travers, P, Walport, M and Schlomchik, MJ (2005). *Immunobiology: The Immune System in Health and Disease*, 6 edn. Garland Science: New York.
- van de Weert, M, Hennink, WE and Jiskoot, W (2000). Protein instability in poly(lactic-co-glycolic acid) microparticles. *Pharm Res* **17**: 1159–1167.
- Cohen, S, Yoshioka, T, Lucarelli, M, Hwang, LH and Langer, R (1991). Controlled delivery systems for proteins based on poly(lactic/glycolic acid) microspheres. *Pharm Res* **8**: 713–720.
- Garlie, NK, LeFever, AV, Siebenlist, RE, Levine, BL, June, CH, Lum, LG (1999). T cells coactivated with immobilized anti-CD3 and anti-CD28 as potential immunotherapy for cancer. *J Immunother* **22**: 336–345.
- Gattinoni, L, Klebanoff, CA, Palmer, DC, Wrzesinski, C, Kerstann, K, Yu, Z *et al.* (2005). Acquisition of full effector function *in vitro* paradoxically impairs the *in vivo* antitumor efficacy of adoptively transferred CD8⁺ T cells. *J Clin Invest* **115**: 1616–1626.
- Oelke, M, Krueger, C, Giuntoli, RL 2nd and Schneck, JP (2005). Artificial antigen-presenting cells: artificial solutions for real diseases. *Trends Mol Med* **11**: 412–420.
- Gopferich, A (1996). Mechanisms of polymer degradation and erosion. *Biomaterials* **17**: 103–114.
- Frank, A (2005). Factors affecting the degradation and drug-release mechanism of poly(lactic acid) and poly[(lactic acid)-co-(glycolic acid)]. *Polymer International* **54**: 36–46.
- Boyman, O, Kovar, M, Rubinstein, MP, Surh, CD and Sprent, J (2006). Selective stimulation of T cell subsets with antibody-cytokine immune complexes. *Science* **311**: 1924–1927.
- Scheffold, A, Murphy, KM and Hofer, T (2007). Competition for cytokines: T(reg) cells take all. *Nat Immunol* **8**: 1285–1287.
- Schneck, JP, Slansky, JE, O’Herrin, SM and Greten, TF (2000). Monitoring antigen specific T-cell using MHC-Ig dimers. In: *Current Protocols in Immunology* John Wiley & Sons. pp. 17.12.11–17.12.17.